

Exploring the potential biomarkers for prognosis of glioblastoma via Weighted Gene Co-expression Network Analysis

Mengyuan Zhang¹, Zhike Zhou², Zhouyang Liu¹, Fangxi Liu¹, Chuansheng Zhao^{Corresp. 1}

¹ Department of Neurology and Stroke Center, The First Hospital of China Medical University, Shenyang, China

² Department of Geriatrics, The First Hospital of China Medical University, Shenyang, China

Corresponding Author: Chuansheng Zhao
Email address: cszhao@cmu.edu.cn

Background: Glioblastoma (GBM) is the most common malignant tumor in the central system with a poor prognosis. Due to the complexity of its molecular mechanism, the recurrence rate and mortality rate of GBM patients are still high. Therefore, there is an urgent need to screen GBM biomarkers to prove the therapeutic effect and improve the prognosis. **Results:** We extracted data from GBM patients from the Gene Expression Integration Database (GEO), analyzed differentially expressed genes in GEO and identified key modules by weighted gene co-expression network analysis (WGCNA). GSE145128 data was obtained from the GEO database, and the darkturquoise module was determined to be the most relevant to the GBM prognosis by WGCNA ($r = -0.62$, $p=0.01$). We performed enrichment analysis of gene ontology (GO) and Kyoto Encyclopedia of Genes and Genomes (KEGG) to reveal the interaction activity in the selected modules. Then Kaplan-Meier survival curve analysis was used to extract genes closely related to GBM prognosis. We used Kaplan-Meier survival curves to analyze the 139 genes in the darkturquoise module, identified four genes (DARS / GDI2 / P4HA2 / TRUB1) associated with prognostic GBM. Low expression of DARS/GDI2/TRUB1 and high expression of P4HA2 had a poor prognosis. Finally, we used tumor genome map (TCGA) data, verified the characteristics of hub genes through Co-expression analysis, Drug sensitivity analysis, TIMER database analysis and GSVA analysis. We downloaded the data of GBM from the TCGA database, the results of co-expression analysis showed that DARS/GDI2/P4HA2/TRUB1 could regulate the development of GBM by affecting genes such as CDC73/CDC123/B4GALT1/CUL2. Drug sensitivity analysis showed that genes are involved in many classic Cancer-related pathways including TSC/mTOR, RAS/MAPK. TIMER database analysis showed DARS expression is positively correlated with tumor purity($cor=0.125, p=1.07e-02$), P4HA2 expression is negatively correlated with tumor purity($cor=-0.279, p=6.06e-09$). Finally, GSVA analysis found that DARS/GDI2/P4HA2/TRUB1 gene sets are closely related to the

occurrence of cancer. Conclusion: We used two public databases to identify four valuable biomarkers for GBM prognosis, namely DARS/GDI2/P4HA2/TRUB1, which have potential clinical application value and can be used as prognostic markers for GBM.

1 **Exploring the potential biomarkers for prognosis of**
2 **glioblastoma via Weighted Gene Co-expression**
3 **Network Analysis**

4 Mengyuan Zhang ¹, Zhike Zhou², Zhouyang Liu¹, Fangxi Liu¹ and Chuansheng Zhao ^{1*}

5 1 Department of Neurology and Stroke Center, The First Hospital of China Medical
6 University, Shenyang 110000, PR China.

7 2 Department of Geriatrics, The First Affiliated Hospital, China Medical University,
8 Shenyang 110000, PR China.

9

10 **Corresponding Author:** Chuansheng Zhao

11 The First Hospital of China Medical University, No. 155 Nanjing North Street, Heping District
12 Shenyang 110000, PR China

13 Email Adress: cszhao@cmu.edu.cn

14

15 **Abstract:**

16 Glioblastoma (GBM) is the most common malignant tumor of the central system, with a poor
17 prognosis. Due to the complexity of its molecular mechanism, the recurrence rate and mortality
18 rate of GBM patients remain high. Therefore, screening of biomarkers for GBM is urgently needed
19 to demonstrate therapeutic efficacy and improve prognosis. In this study, we extracted GBM
20 patients' data from gene expression integration database (GEO), analyzed the differentially
21 expressed genes in GEO by Weighted gene co-expression network analysis (WGCNA),
22 constructed the co-expression network, and determined the correlation with the key recurrent
23 modules of GBM. At the same time, based on Gene Ontology (GO) and Kyoto Encyclopedia of
24 Genes and Genomes (KEGG), the selected modules were analyzed. Then four genes (DARS /
25 GDI2 / P4HA2 / TRUB1) which are closely related to the prognosis of GBM were extracted by
26 Kaplan-Meier survival curve analysis. The characteristics of these four genes were verified by
27 tumor genome atlas (TCGA) data, Co-expression analysis, Drug sensitivity analysis, TIMER
28 database analysis and Gene set variation analysis (GSVA) analysis. It was found that these four
29 genes were differentially expressed genes in the initiation and progression of GBM, which could
30 provide reference and basis for the observation of the clinical treatment and prognosis of GBM.

31

32 **Introduction**

33 Glioblastoma (GBM) is the most common primary neurogenic tumor, and the prognosis of most
34 subtypes is poor (Tan et al. 2020). Despite of aggressive treatment strategies such as surgery
35 followed by irradiation and chemotherapy, the prognoses of GBM patients remained unsatisfactory
36 (Wu et al. 2020). According to the existing data, GBM patients have a survival of only 12–15
37 months after the standard treatment, with the 5-year survival rate of 3–5% (Gong et al. 2020; Szopa
38 et al. 2017). The main reasons for the poor prognosis of GBM are due to tumor metastasis and
39 postoperative recurrence (Tij et al. 2021). Given that tumors invade the brain aggressively, GBM
40 tumors can rarely be completely removed by surgery (Reichel et al. 2020). And the resulting
41 network by GBM enables multicellular communication through microtubule-associated gap
42 junctions, and increases tumor resistance to cell ablation and radiotherapy (Li et al. 2017a).
43 Actively searching for biological markers related to the treatment and prognosis of GBM patients
44 is of great significance for improving the survival rate of GBM patients.

45 In the past few decades, gene sequencing and bioinformatics analysis have been widely used for
46 genetic variation screening at the gene level (Tingting et al. 2019), which helps us to identify
47 differentially expressed genes (DEG) and functional pathways in the development of GBM. It has
48 been found that the increased expression of SPRY2 mRNA indicates the decreased survival rate
49 of GBM patients (Li et al. 2017a). Another study showed that the mRNA levels of NOTCH and
50 Epidermal Growth Factor Receptor (EGFR) genes were increased in GBM tissues, which was
51 related to the survival of patients (Irshad et al. 2015; Xing et al. 2015). However, most of these
52 studies are single gene analysis, which may limit the analysis of the pathogenesis and prognosis
53 of GBM.

54 Weighted gene co-expression network analysis (WGCNA) is a platform to identify hub genes or
55 therapeutic targets based on the interconnectivity of gene subsets and the association between gene
56 subsets and phenotypes (Wang et al. 2020; Zhang & Horvath 2005). WGCNA can use the
57 information of thousands of genes to identify the gene modules of interest and perform important

58 association analysis on phenotypes. Recently, many journals have published relevant studies using
59 WGCNA(Schafer et al. 2019; Wang et al. 2020; Zhou et al. 2018).

60 In this study, we extracted four GBM related biomarkers (DARS / GDI2 / P4HA2 / TRUB1) by
61 extracting data from GBM patients from the gene expression integrated database (GEO) and using
62 WGCNA and Kaplan-Meier survival curves analysis. Then, we established GBM gene markers in
63 the tumor genome atlas (TCGA), and confirmed the characteristics of these four genes by means
64 of Co-expression analysis, Drug sensitivity analysis, TIMER database analysis , and GSVA
65 analysis. In summary, our purpose is to find reliable biomarkers related to the prognosis of GBM
66 by analyzing the relationship between DARS / GDI2 / P4HA2 / TRUB1 gene and GBM, so as to
67 provide reference and basis for clinical treatment and prognosis observation of GBM.

68 **Materials and methods**

69 ***Data information and construction of WGCNA***

70 The Series Matrix File data File of GSE145128 was downloaded from the NCBI GEO public
71 database, which were contained 15 GBM patients and sets of transcriptional data, including
72 untreated group (n=7) and recurrent group (n=8), for the construction of WGCNA co-expression
73 network.

74 We constructed a weighted gene co-expression network to find co-expressed gene modules, and
75 clarified the relationship between the gene network and phenotype and hub genes. The WGCNA-
76 R package was used to construct a co-expression network of genes in the GSE145128 dataset,
77 where the soft-thresholding power was set to 16. The weighted adjacency matrix is converted into
78 a topological overlap matrix (TOM) to estimate the network connectivity, and a hierarchical
79 clustering method is used to construct a clustering tree structure of the TOM matrix. Different gene
80 modules are represented by different cluster tree branches and colors. All genes are divided into
81 multiple modules through gene expression patterns, and genes with similar expression patterns are
82 divided into one module based on weighted correlation coefficients and expression patterns.

83 ***Enrichment analysis of gene module function***

84 In order to obtain the biological functions and signaling pathways involved in the interest module
85 of WGCNA, the Metascape database (www.metascape.org) was used for annotation and
86 visualization, and Gene Ontology (GO) analysis and Kyoto Encyclopedia of Genes and Genomes
87 (KEGG) pathway enrichment analyses were performed on the genes in the specific module. Min
88 overlap ≥ 3 & $p \leq 0.01$ was considered statistically significant.

89 ***Identifying Hub Genes***

90 To determine hub genes, the most important thing is whether they have an impact on tumor
91 prognosis. According to WGCNA theory, hub genes have the highest connectivity in the module,
92 which determines the biological significance of the module(Chen et al. 2019). So we think that
93 hub genes must exist in the interested module of WGCNA. Combined with the above two points,
94 we analyzed the Kaplan-Meier survival rate of all genes in the interest module of WGCNA. We

95 believe that the genes that can affect the prognosis of GBM patients are the hub genes. And then, the
96 next step is to explore and verify the specific molecular mechanism of hub genes.

97 ***Download and Pre-processing Data From TCGA***

98 TCGA database as the biggest cancer gene information database, including gene expression data,
99 the miRNA expression data and copy number variation, DNA methylation, SNPS and other data.
100 We downloaded the processed original mRNA expression data of GBM. A total of 159 specimens
101 were collected (Supplementary table S1).

102 ***Co-expression analysis***

103 The co-expression of the hub genes were analyzed. The correlation coefficient filter condition
104 was 0.3 and the p-value was 0.001. After screening the genes with the most significant
105 expression of hub genes, the correlation analysis circles of hub genes were plotted using
106 "corrplot" and "circlize" packages.

107 ***GSCALite and GDSC***

108 GSCALite is a set analysis platform for cancer genes. It integrates cancer genomics data of 33
109 cancer types from TCGA, drug response data from GDSC and CTRP, and normal tissue data
110 from GTEx, and conducts gene set analysis in the data analysis process. Our study through this
111 analysis was carried out on the hub genes. Then based on the largest publicly available
112 pharmacogenomics database (GDSC, the Genomics of Drug Sensitivity in Cancer,
113 <https://www.cancerrxgene.org/>), we used the R packet "pRophetic" to predict the
114 chemosensitivity of each tumor sample, and the estimated IC₅₀ of each specific
115 chemotherapeutic drug treatment was obtained by ridge regression. The prediction accuracy was
116 measured by 10-fold cross-validation with the GDSC training set. Select default values for all
117 parameters, including "combats" to remove batch effects, "allSoldTumours" for tissue types, and
118 average values for summarizing repetitive gene expressions (Liu et al. 2018).

119 ***TIMER database analysis***

120 TIMER is a website for systematically testing the molecular characteristics of tumor-immune
121 interactions (Li et al. 2017b). This website has incorporated 10,897 samples ranging from 32
122 different kinds of cancer types from the TCGA dataset (Shi et al. 2020). In this study, TIMER was
123 used to explore the relationship between hub genes and the contents of immune cells and to
124 compare the infiltration levels between tumors with different somatic copy number changes of hub
125 genes.

126 ***Gene functional analysis***

127 GSVA uses a non-parametric and unsupervised method, and bypasses the traditional method of
128 explicitly modeling phenotypes in affluent scoring algorithms (Hanzelmann et al. 2013). By

129 comprehensively scoring the gene set of interest, GSVA converts the gene level change into the
130 pathway level change, and then judges the biological function of the sample. In this study, the gene
131 sets were downloaded from the Molecular signatures database (v7.0 version), and used the
132 algorithm of GSVA comprehensive score of each gene set, evaluating the potential biological
133 function change different samples.

134 **Statistical analysis**

135 All statistical analyses were performed in R language (version 3.6). All the statistical tests were
136 bilateral, and $p < 0.05$ was statistically significant.

137

138 **Result**

139 **Identification of gene co-expression modules**

140 The Series Matrix File data File of GSE145128 was downloaded from the NCBI GEO public
141 database. A total of 15 transcriptional data sets, including untreated group ($n=7$) and recurrent
142 group ($n=8$), were used to construct the WGCNA co-expression network. In order to determine
143 whether the 15 samples in GSE145128 were suitable for network analysis, a sample dendrogram
144 and similar clinical features were studied. We confirmed that all samples were included in the
145 group (Fig. 1A). The soft-thresholding power was set as 16 for the subsequent construction of co-
146 expression network (Fig. 1B, Fig. 1C). The clustering tree structure of TOM matrix was
147 constructed by hierarchical clustering method. The different branches and colors represent
148 different gene modules (Fig. 1D). The network heatmap was used to analyze the interaction of 41
149 modules (Fig. 1E). The results showed that each module was independent of each other, indicating
150 that each module was highly personalized and the gene expression of each module was relatively
151 independent.

152 **Correlation of modules and clinical traits**

153 In order to study the relationship between these modules and the prognosis of GBM, we
154 investigated the correlation between each module and the prognosis of GBM. We found that the
155 darkturquoise module had the highest correlation with disease relapse ($r = -0.62$, $p = 0.01$) (Fig.
156 2A, B). We used Metascape to analyze the function and pathway of the darkturquoise module.
157 Metascape can identify the enrichment process in the gene list and the association between
158 enrichment processes [14, 15] by querying many databases, such as GO functional, Hallmark Gene
159 Sets, and KEGG pathways (Tripathi et al. 2015; Zheng et al. 2018). Based on GO enrichment
160 analysis, it was found that the co-expressed genes within the modules of interest s mainly related
161 to the steady state of cellular transition metal ion homeostasis, protein hydroxylation, intrinsic
162 apoptotic signaling pathway, ncRNA metabolic process (Fig. 2C). The KEGG pathway analysis
163 revealed that the co-expressed genes within the modules of interest was mostly enriched in the
164 'Ferroptosis' (Fig. 2C). In addition, the enrichment processes were highly connected and could be
165 clustered into a complete network (Fig. 2C). These results indicated that these functions were
166 related in the occurrence and development of GBM.

167 **Identification of hub genes in darkturquoise module**

168 According to the WGCNA theory, hub genes have the highest connectivity in the module, which
169 determine the biological significance of the module (Chen et al. 2019). Therefore, we searched for
170 hub genes in the darkturquoise module. We analyzed the Kaplan-Meier survival curves of 139
171 genes in the darkturquoise module. 14 genes with significant survival analysis results ($p < 0.05$)
172 were selected for sequencing (Table. 1). Finally, we found that only four genes
173 (DARS/GDI2/P4HA2/TRUB1) had an impact on the prognosis of GBM patients (Fig. 3). Survival
174 analysis showed that the patients with low expression of DARS/GDI2/ TRUB1 and high
175 expression of P4HA2 had poor prognosis.

176

177 **Analysis of the co-expression of hub genes**

178 It was clear that the hub genes can affect the process of disease progression by regulating related
179 genes. It can be assumed that DARS/GDI2/P4HA2/TRUB1 was associated with the most abundant
180 pathways and genes and could regulate more biological processes. In order to assess the gene
181 correlation of DARS / GDI2 / P4HA2 / TRUB1, we analyzed the co-expression of
182 DARS/GDI2/P4HA2/TRUB1 through Pearson correlation analysis ($\text{cor} > 0.3$, $p < 0.001$). We
183 screened the 10 genes with the strongest correlation with the expression of DARS / GDI2 / P4HA2
184 / TRUB1, drew the correlation analysis map and heat map of DARS / GDI2 / P4HA2 / TRUB1
185 (Fig. 4A-4H), and found that the correlation between DARS and CDC73 was the highest, and the
186 correlation between GDI2 and CDC123 was the highest. P4HA2 and B4GALT1 have the highest
187 correlation, TRUB1 and CUL2 have the highest correlation (Fig. 4I-L). Among them, CDC73 and
188 CDC123 are cyclins of cell division (Sun et al.), B4GALT1 is one of seven β - 1, 4-
189 galactosyltransferases (B4GALT). CUL2 contributes to form E3 ubiquitin ligase that can
190 recognize numerous substrates and is involved in a variety of cellular processes (Liu et al. 2019).
191 These four genes have been shown to have a close relationship with many kinds of cancers (Cao et
192 al. 2020a; Dou et al. 2020; Li et al. 2019a), such as thyroid carcinoma (Sarquis et al. 2019), breast
193 cancer, etc.

194

195 **Cancer-related pathways and drug sensitivity analysis of hub genes.**

196 First, we investigated the role of hub genes in all well-known cancer-related pathways, as the
197 following: TSC/mTOR, RTK, RAS/MAPK, PI3K/AKT, Hormone ER, Hormone AR, EMT, DNA
198 Damage Response, Cell Cycle, Apoptosis pathways. The results found that DARS participated in
199 the TSC/mTOR pathway activation; GDI2 was involved in Apoptosis, TSC/mTOR pathway
200 activation; P4HA2 was involved in DNA Damage Response, EMT, Hormone AR, Hormone ER,
201 RAS/MAPK and TSC/mTOR pathway; TRUB1 was involved in Apoptosis, DNA Damage
202 Response, EMT, Hormone AR, PI3K/AKT and TSC/mTOR pathway (Fig. 5A). To investigate
203 whether the expression of DARS / GDI2 / P4HA2 / TRUB1 in GBM had an impact on treatment
204 (e.g. chemotherapies), we constructed a predictive model on six commonly used chemo drugs (i.e.

205 AKT.inhibitor, Cisplatin, Dasatinib, Erlotinib, Gefitinib, and Gemcitabine) and confirmed that
206 high expression of DARS was less sensitive to Cisplatin($p=0.00026$) and Gemcitabine($p=0.0024$),
207 high expression of GDI2 was less sensitive to AKT.inhibitor($p=5.2e-05$), Cisplatin($p=0.00067$),
208 Dasatinib($p=0.012$) and Gemcitabine($p=3.5e-06$), low expression of P4HA2 was less sensitive to
209 Cisplatin($p=0.0032$), and Gemcitabine($p=0.00017$),and high expression of TRUB1 was less
210 sensitive to AKT.inhibitor($p=0.00043$)(Fig.5B).

211

212 ***Immune cells infiltration analysis***

213 In view of the obvious prognostic value of DARS/GDI2/P4HA2/TRUB1 gene, we used the
214 TIMER database to determine whether there was an association between tumor-infiltrating and
215 immune cells and DARS/GDI2/P4HA2/TRUB1 expression. Results showed that DARS expression
216 was positively correlated with tumor purity, P4HA2 and B cells (partial $cor=-0.239$, $p=7.89e-07$),
217 P4HA2 and CD8+ T cells (partial $cor=-0.158$, $p=1.19e-03$), TRUB1 and CD8+ T cells (partial
218 $cor=-0.206$, $p=1.87e-02$), DARS and neutrophils (partial $cor= 0.245$, $p=3.73e-07$), GDI2 and
219 neutrophils (partial $cor=0.184$, $p=1.62e-04$), GDI2 and Dendritic cells (partial $cor=0.167$, $p=6.21e-$
220 04) P4HA2 and B cells (partial $cor=-0.239$, $p=7.89e-07$), P4HA2 and CD8+ T cells (partial $cor=-$
221 0.158 , $p=1.19e-03$), TRUB1 and CD8+ T cells (partial $cor=-0.206$, $p=1.87e-02$), DARS and
222 neutrophils (partial $cor= 0.245$, $p=3.73e-07$), GDI2 and neutrophils (partial $cor=0.184$, $p=1.62e-$
223 04), GDI2 and Dendritic cells (partial $cor=0.167$, $p=6.21e-04$) (Fig. 6A). We also explored the
224 correlation between tumor immune cell infiltration and somatic copy number alterations (SCNAs).
225 The samples were divided into four types according to the copy number of genes. The distribution
226 of infiltrating immune cells among the four types of samples was compared, as shown in Fig. 6B.
227 We found that the various forms of mutations carried by the DARS / GDI2 / P4HA2 / TRUB1
228 gene can usually suppress immune infiltration, including CD8+T cells, neutrophils, dendritic cells,
229 macrophages, CD4+T cells, and B cells. Also, we found that these four pivotal genes had a greater
230 effect on immune infiltration than alterations in the genes.

231

232 ***Genomic alterations of DARS/GDI2/P4HA2/TRUB1 in GBM***

233 We then used the cBioPortal tool to determine the types and frequency of
234 DARS/GDI2/P4HA2/TRUB1 alterations based on DNA sequencing data from GBM patients. The
235 genetic variation rates of DARS/GDI2/P4HA2/TRUB1 ranged from 0% to 4% (DARS was 4%,
236 GDI2 was 1.4%, P4HA2 was 4%, TRUB1 was 0.0%.) These alterations include Missense
237 Mutation, mRNA High, mRNA Low, Amplification (AMP), and Deep Deletion.(Fig. 7) In view
238 of this, DARS and P4HA2 show potentially stronger cancer-driving properties at a higher mutation
239 frequency. In contrast, TRUB1 is genetically stable and could potentially act as a stable biomarker.

240

241 ***Gene functional analysis***

242 We downloaded the DARS/GDI2/P4HA2/TRUB1 gene sets from the Molecular signatures
243 database (v7.0 version) and comprehensively evaluated the gene sets through GSVA. Our analysis
244 showed that in the DARS gene set, 17 gene sets were up-regulated ($t > 1$) and 14 gene sets were
245 down-regulated ($t < 1$). In GDI2, 13 gene sets were up-regulated and 21 gene sets were down-
246 regulated. In P4HA2, 11 gene sets were up-regulated and 30 gene sets were down-regulated. In
247 TRUB1, 21 gene sets were down-regulated and 14 gene sets were down-regulated. (Fig. 8A - D).

248

249 Discussion

250 Due to the complex mechanisms of GBM, it is one of the most threatening CNS malignancies.
251 Therefore, it is an urgent need to find biomarkers related to the occurrence and prognosis of GBM
252 to reveal the possible pathogenesis or predict the prognosis of patients, and then develop
253 personalized treatment plans for GBM patients. Based on gene sequencing technology, we have
254 discovered some biological markers with predictive value for patients including GBM. However,
255 the role of these markers are still limited. In order to better understand GBM, there is an urgent
256 need to screen out more biomarkers to improve the efficacy of GBM treatment and prognosis.

257 GBM, as a highly heterogeneous tumor harboring multiple genetic alterations (Harter et al.
258 2014), molecular heterogeneity affects the effectiveness of single-molecule markers in predicting
259 prognosis (Tonry 2020). At the same time, some studies have found that the high recurrence rate
260 of GBM is related to the expression of strong proliferation genes of cells (Lara-Velazquez et al.
261 2020). And these processes usually involve multiple genes (Malik et al. 2020). Therefore, we
262 believe that multi-gene markers have a higher predictive power for GBM prognosis than single-
263 gene marker. We built a multi-gene markers model for predicting GBM prognosis, and validated
264 the multi-gene markers model through strategies including training, testing, and independent cross-
265 validation. The above strategies significantly improve the predictive ability of genetic markers (Li
266 et al. 2019b).

267 In our research and analysis, the results of GO and KEGG analysis indicate that cell transition
268 metal ion homeostasis, protein hydroxylation, intrinsic apoptotic signaling pathway and other
269 processes may play an important role in GBM. Among them, transition metals are critical for
270 many metabolic processes (Nelson & N. 2014), and their steady state is vital to life. Aberrations in
271 the cellular metal ion concentrations may lead to cell death and severe diseases such as cancer (Pi
272 et al. 2020). Hydroxylation is a post-translational modification affecting protein stability, activity
273 or interactome (Zurlo & Zhang 2020). Many cancers are related to protein hydroxylation, such as
274 breast cancer (Zurlo & Zhang 2020), gastric cancer (Li et al. 2020), and prostate cancer (Della-Flora
275 et al. 2020). For example, a study found that a set of enzymes PLOD1, PLOD2 and PLOD3
276 involved in the hydroxylation of lysine and stabilization of collagen by crosslinks, which up-
277 regulated expression in gastric cancer patients (Li et al. 2020). Similarly, intrinsic apoptotic
278 signaling pathway can activate or inactivate multiple signaling pathways and inhibit multiple
279 tumor suppressor genes, thereby promoting tumor progression. Almost all cancers involve intrinsic
280 apoptotic signaling pathway, including renal cell carcinoma (Chae et al. 2020) and multiple
281 myeloma (Chen et al. 2020a). Combined with the above results, we believe that DARS / GDI2 /
282 P4HA2 / TRUB1 may be involved in these processes to affect the occurrence and development of
283 GBM disease, which is also consistent with our Drug sensitivity analysis results. Among them, the
284 DARS gene encodes the aspartyl-tRNA synthetase (Dominik et al. 2018), which pairs aspartate

285 with its corresponding tRNA. Missense mutations in the gene encoding DARS can lead to
286 leukocyte dystrophy, accompanied by a marked reduction in myelin sheath, abnormal movement
287 and cognitive impairment (Fröhlich et al. 2018). There are no related reports about the relations
288 between DARS and GBM. According to our research, DARS may participate in TSC/mTOR
289 signaling, by regulating GBM cell growth process. GDI2 controls the activity of Rho GTPase's
290 pathway to regulatory guanine nucleotide exchange factor and GTPase activating protein, and may
291 play a role in tumor cell apoptosis. This is also in line with our results. At the same time, a recent
292 study shows that RhoGDI2 suppresses lung metastasis in mice by reducing tumor versican
293 expression and macrophage infiltration. The expression of P4HA2 increased in head and neck
294 squamous cell carcinoma (HNSCC)(Kisoda et al. 2020), Oral Squamous Cell Carcinoma
295 (OSCC)(Reis et al. 2020), cervical cancer(Cao et al. 2020b) and other cancers. Especially, we
296 found that P4HA2 are markedly upregulated in cervical cancer tissues and upregulation of P4HA2
297 was associated with shorter overall survival (OS) and relapse-free survival (RFS)(Cao et al.
298 2020b). In GBM, we found that P4HA2 is mainly involved in the process of inhibiting DNA
299 damage, and is also related to EMT, Hormone AR, Hormone ER, RAS / MAPK, TSC / mTOR
300 and other pathways. TRUB1 mRNA is widely expressed in various human tissues (especially
301 heart, skeletal muscle and liver), but there are few studies on its relationship with cancer(Zucchini
302 et al. 2003). In our research, we analyzed that TRUB1 is mainly involved in Apoptosis, DNA
303 damage, EMT, PI3K / AKT and other processes.

304 In the analysis of hub genes co-expression, we found the four genes (CDC73 / CDC123 /
305 B4GALT1 / CUL2) are most relevant to the expression of hub genes and also related to the
306 occurrence of many cancers. For example, CDC73 is a tumor suppressor, which can prevent cells
307 from growing and dividing too fast or uncontrolled, and is closely related to parathyroid
308 carcinoma(Cetani et al. 2019). CDC123 is a cell division cycle protein, and the regulatory effects
309 of the entire cell cycle process can be stopped in one of the normal stages (G1, S, G2, M).CDC123
310 is highly expressed in choriocarcinoma(Hussain et al. 2018). B4GALT1 is one of the seven β -1,4-
311 galactosyltransferase (beta4galt) genes. The β 1,4-galactosylation of glycans is very important for
312 many biological events, including the development of cancer. In a variety of cancers, the
313 B4GALTs family is associated with cancer cell proliferation, invasion, metastasis, and drug
314 resistance.B4GALT1 is highly expressed in patients with lung adenocarcinoma(Zhang et al. 2019).
315 CUL2is one of the seven members of Cullin family. It can participate in the regulation of cell
316 cycle, proliferation, apoptosis, differentiation, gene expression, transcription regulation, signal
317 transmission, damage repair, inflammation and immunity.CUL2 affects the occurrence of renal
318 cell carcinoma by promoting the substrate ubiquitination and degradation(Liu et al. 2020).

319 Further TIMER analysis indicated that the immune system had a good effect on tumor
320 microenvironment, and that the mutations of DARS / GDI2 / P4HA2 / TRUB1 had important
321 application value in tumor immunology. Finally, we conducted a comprehensive evaluation of
322 gene sets using GSEA and we found that the DARS/GDI2/P4HA2/TRUB1 gene sets are closely
323 related to the occurrence of cancer.For instance, the APICAL_ JUNCTION in the DARS gene set
324 is more common in highly differentiated epithelial cells, such as colon cancer cells(Nair-Menon et
325 al. 2020).MITOTIC_SPINDLE in the GDI2 gene set, the mitotic spindle inhibitor is one of the
326 most commonly used chemotherapeutics now(Bukowski et al. 2020). DNA_REPAIR in the
327 P4HA2 gene set and ANGIOGENESIS in the TRUB1 gene set are also two important mechanisms
328 of cancer development .

329 In recent years, with the GBM genes related to the occurrence and prognosis of feature
330 recognition in many studies. Such as Chen X found the ASPM expression pattern from the database
331 showed that it is highly expressed in GBM tissue, and patients with high expression of ASPM have
332 a poor prognosis (Chen et al. 2020b). Recently, a bioinformatic analysis of 123 GBM patients has
333 established a 14-mRNA prognostic signature, which could be used to classify GBM patients into
334 low and high risk groups (Arimappamagan et al. 2013). To our knowledge, the
335 DARS/GDI2/P4HA2/TRUB1 that we identified are new GBM biomarkers because they have
336 never been reported to be associated with the development and progression of GBM (Lu et al.
337 2020). At the same time, compared with the traditional typing methods, the multi-gene markers
338 model has many advantages, such as high prediction accuracy and personalized detection
339 results (Albuquerque et al. 2012). Therefore, multi-gene markers have a good application prospect
340 in clinical practice. In our study, we built and verified the characteristic of the four genes through
341 analyzing the two independent data sets. More reasonable use of biometrics and multiple
342 independent data sets of mutual verification makes our results more reliable.

343 However, our study had some limitations. Associated with disease, for example, age, race,
344 sex, and some unknown prognostic factors may not be included in the model, which limits the
345 prediction ability of the model. In the future, we plan to establish a more reasonable model of
346 biological information analysis. Meanwhile, it should be acknowledged that the single gene
347 analysis in this study does have limitations, and in future studies we will combine all the hub genes
348 or other factors together to find a biomarker with better sensitivity and accuracy using a multi-
349 omics approach. In summary, our results had shown that DARS/GDI2/P4HA2/TRUB1 can be used
350 as a new biological marker for GBM, which is related to the occurrence and prognosis of GBM,
351 how to rationally apply various genetic characteristics at specific stages of GBM for diagnose and
352 prediction of prognosis.

353 Conclusion

354 The molecular biological characteristics of GBM has changed the classification and treatment of
355 tumors and become an important part of diagnosis and oncologic therapy. This study used public
356 databases to identify four valuable biomarkers for GBM prognosis, namely DARS / GDI2 / P4HA2
357 / TRUB1, which have potential and clinical application values to act as prognostic markers of
358 GBM.

359

360 Acknowledgement

361 None

362 Reference

363 Albuquerque AD, Kubisch I, Breier G, Stamminger G, Fersis N, Eichler A, Kaul S, and St?Lzel
364 U. 2012. Multimarker gene analysis of circulating tumor cells in pancreatic cancer patients: a
365 feasibility study. *Oncology* 82:3-10.

366 Arimappamagan A, Somasundaram K, Thennarasu K, Peddagangannagari S, Srinivasan H,
367 Shailaja BC, Samuel C, Patric IR, Shukla S, Thota B, Prasanna KV, Pandey P, Balasubramaniam
368 A, Santosh V, Chandramouli BA, Hegde AS, Kondaiah P, and Sathyanarayana Rao MR. 2013. A

- 369 fourteen gene GBM prognostic signature identifies association of immune response pathway and
370 mesenchymal subtype with high risk group. *PLoS ONE* 8:e62042. 10.1371/journal.pone.0062042
- 371 Bukowski K, Kciuk M, and Kontek R. 2020. Mechanisms of Multidrug Resistance in Cancer
372 Chemotherapy. *Int J Mol Sci* 21. 10.3390/ijms21093233
- 373 Cao Y, Han Q, Li J, Jia Y, and Shi H. 2020a. P4HA2 contributes to cervical cancer progression
374 via inducing epithelial-mesenchymal transition. *Journal of Cancer* 11:2788-2799.
- 375 Cao Y, Han Q, Li J, Jia Y, Zhang R, and Shi H. 2020b. P4HA2 contributes to cervical cancer
376 progression via inducing epithelial-mesenchymal transition. *J Cancer* 11:2788-2799.
377 10.7150/jca.38401
- 378 Cetani F, Marcocci C, Torregrossa L, and Pardi E. 2019. Atypical parathyroid adenomas:
379 challenging lesions in the differential diagnosis of endocrine tumors. *Endocr Relat Cancer*
380 26:R441-R464. 10.1530/ERC-19-0135
- 381 Chae IG, Song NY, Kim DH, Lee MY, Park JM, and Chun KS. 2020. Thymoquinone induces
382 apoptosis of human renal carcinoma Caki-1 cells by inhibiting JAK2/STAT3 through pro-oxidant
383 effect. *Food Chem Toxicol* 139:111253. 10.1016/j.fct.2020.111253
- 384 Chen G, Hu K, Sun H, Zhou J, Song D, Xu Z, Gao L, Lu Y, Cheng Y, Feng Q, Zhang H, Wang
385 Y, Hu L, Lu K, Wu X, Li B, Zhu W, and Shi J. 2020a. A novel phosphoramidate compound,
386 DCZ0847, displays in vitro and in vivo anti-myeloma activity, alone or in combination with
387 bortezomib. *Cancer Lett* 478:45-55. 10.1016/j.canlet.2020.03.006
- 388 Chen L, Peng T, Luo Y, Zhou F, Wang G, Qian K, Xiao Y, and Wang X. 2019. ACAT1 and
389 Metabolism-Related Pathways Are Essential for the Progression of Clear Cell Renal Cell
390 Carcinoma (ccRCC), as Determined by Co-expression Network Analysis. *Front Oncol* 9:957.
391 10.3389/fonc.2019.00957
- 392 Chen X, Huang L, Yang Y, Chen S, Sun J, Ma C, Xie J, Song Y, and Yang J. 2020b. ASPM
393 promotes glioblastoma growth by regulating G1 restriction point progression and Wnt-beta-
394 catenin signaling. *Aging (Albany NY)* 12:224-241. 10.18632/aging.102612
- 395 Della-Flora A, Wilde ML, Pinto IDF, Lima EC, and Sirtori C. 2020. Degradation of the anticancer
396 drug flutamide by solar photo-Fenton treatment at near-neutral pH: Identification of transformation
397 products and in silico (Q)SAR risk assessment. *Environ Res* 183:109223.
398 10.1016/j.envres.2020.109223
- 399 Dominik F, Suchowerska AK, Carola V, He R, Ernst W, Georg VJ, Cas S, Thomas F, Housley
400 GD, and Matthias K. 2018. Expression Pattern of the Aspartyl-tRNA Synthetase DARS in the
401 Human Brain. *Frontiers in Molecular Neuroscience* 11:81-.
- 402 Dou B, Jiang Z, Chen X, Wang C, and Sheng G. 2020. Oncogenic Long Noncoding RNA DARS-
403 AS1 in Childhood Acute Myeloid Leukemia by Binding to microRNA-425. *Technology in Cancer*
404 *Research & Treatment* 19:153303382096558.
- 405 Fröhlich D, Suchowerska AK, Voss C, He R, Wolvetang E, von Jonquieres G, Simons C, Fath T,
406 Housley GD, and Klugmann M. 2018. Expression Pattern of the Aspartyl-tRNA Synthetase DARS
407 in the Human Brain. *Frontiers in Molecular Neuroscience* 11. 10.3389/fnmol.2018.00081

- 408 Gong Z, Hong F, Wang H, Zhang X, and Chen J. 2020. An eight-mRNA signature outperforms
409 the lncRNA-based signature in predicting prognosis of patients with glioblastoma. *BMC Med*
410 *Genet* 21:56. 10.1186/s12881-020-0992-7
- 411 Hanzelmann S, Castelo R, and Guinney J. 2013. GSEA: gene set variation analysis for microarray
412 and RNA-seq data. *BMC Bioinformatics* 14:7. 10.1186/1471-2105-14-7
- 413 Harter D, Wilson T, and Karajannis M. 2014. Glioblastoma multiforme: State of the art and future
414 therapeutics. *Surgical Neurology International* 5. 10.4103/2152-7806.132138
- 415 Hussain S, Saxena S, Shrivastava S, Mohanty AK, Kumar S, Singh RJ, Kumar A, Wani SA,
416 Gandham RK, Kumar N, Sharma AK, Tiwari AK, and Singh RK. 2018. Gene expression profiling
417 of spontaneously occurring canine mammary tumours: Insight into gene networks and pathways
418 linked to cancer pathogenesis. *PLoS ONE* 13:e0208656. 10.1371/journal.pone.0208656
- 419 Irshad K, Mohapatra SK, Srivastava C, Garg H, Mishra S, Dikshit B, Sarkar C, Gupta D, Chandra
420 PS, Chattopadhyay P, Sinha S, and Chosdol K. 2015. A combined gene signature of hypoxia and
421 notch pathway in human glioblastoma and its prognostic relevance. *PLoS ONE* 10:e0118201.
422 10.1371/journal.pone.0118201
- 423 Kisoda S, Shao W, Fujiwara N, Mouri Y, Tsunematsu T, Jin S, Arakaki R, Ishimaru N, and Kudo
424 Y. 2020. Prognostic value of partial EMT-related genes in head and neck squamous cell carcinoma
425 by a bioinformatic analysis. *Oral Dis*. 10.1111/odi.13351
- 426 Lara-Velazquez M, Zarco N, Carrano A, Phillipps J, and Guerrero-Cazares H. 2020. 543:
427 Cerebrospinal Fluid-Responsive Factor SERPINA3 Promotes Proliferation, Migration and
428 Invasion of Glioblastoma. 543: Cerebrospinal Fluid-Responsive Factor SERPINA3 Promotes
429 Proliferation, Migration and Invasion of Glioblastoma.
- 430 Li C, Tan J, Chang J, Li W, Liu Z, Li N, and Ji Y. 2017a. Radioiodine-labeled anti-epidermal
431 growth factor receptor binding bovine serum albumin-polycaprolactone for targeting imaging of
432 glioblastoma. *Oncol Rep* 38:2919-2926. 10.3892/or.2017.5937
- 433 Li Q, Wang Q, Zhang Q, Zhang J, and Zhang J. 2019a. Collagen prolyl 4-hydroxylase 2 predicts
434 worse prognosis and promotes glycolysis in cervical cancer. *American Journal of Translational*
435 *Research* 11:6938-6951.
- 436 Li SS, Lian YF, Huang YL, Huang YH, and Xiao J. 2020. Overexpressing PLOD family genes
437 predict poor prognosis in gastric cancer. *J Cancer* 11:121-131. 10.7150/jca.35763
- 438 Li T, Fan J, Wang B, Traugh N, Chen Q, Liu JS, Li B, and Liu XS. 2017b. TIMER: A Web Server
439 for Comprehensive Analysis of Tumor-Infiltrating Immune Cells. *Cancer Research* 77:e108-e110.
440 10.1158/0008-5472.Can-17-0307
- 441 Li W, Lu J, Ma Z, Zhao J, and Liu J. 2019b. An Integrated Model Based on a Six-Gene Signature
442 Predicts Overall Survival in Patients With Hepatocellular Carcinoma. *Front Genet* 10:1323.
443 10.3389/fgene.2019.01323
- 444 Liu A, Zhang S, Shen Y, Lei R, and Wang Y. 2019. Association of mRNA expression levels of
445 Cullin family members with prognosis in breast cancer. *Medicine* 98.
446 10.1097/md.00000000000016625

- 447 Liu CJ, Hu FF, Xia MX, Han L, Zhang Q, and Guo AY. 2018. GSCALite: a web server for gene
448 set cancer analysis. *Bioinformatics* 34:3771-3772. 10.1093/bioinformatics/bty411
- 449 Liu X, Zurlo G, and Zhang Q. 2020. The Roles of Cullin-2 E3 Ubiquitin Ligase Complex in
450 Cancer. *Adv Exp Med Biol* 1217:173-186. 10.1007/978-981-15-1025-0_11
- 451 Lu WC, Xie H, Yuan C, Li JJ, and Wu AH. 2020. Identification of potential biomarkers and
452 candidate small molecule drugs in glioblastoma. *Cancer Cell International* 20.
- 453 Malik V, Garg S, Afzal S, Dhanjal JK, and Wadhwa R. 2020. Bioinformatics and Molecular
454 Insights to Anti-Metastasis Activity of Triethylene Glycol Derivatives. *International Journal of*
455 *Molecular Sciences* 21.
- 456 Nair-Menon J, Daulagala AC, Connor DM, Rutledge L, Penix T, Bridges MC, Wellslager B,
457 Spyropoulos DD, Timmers CD, Broome AM, and Kourtidis A. 2020. Predominant Distribution of
458 the RNAi Machinery at Apical Adherens Junctions in Colonic Epithelia Is Disrupted in Cancer.
459 *Int J Mol Sci* 21. 10.3390/ijms21072559
- 460 Nelson, and N. 2014. Metal ion transporters and homeostasis. *Embo Journal* 18:4361-4371.
- 461 Pi H, Wendel BM, and Helmann JD. 2020. Dysregulation of Magnesium Transport Protects
462 *Bacillus subtilis* against Manganese and Cobalt Intoxication. *J Bacteriol* 202. 10.1128/JB.00711-
463 19
- 464 Reichel D, Sagong B, Teh J, Zhang Y, and Perez JM. 2020. Near Infrared Fluorescent
465 Nanoplatfom for Targeted Intraoperative Resection and Chemotherapeutic Treatment of
466 Glioblastoma. *ACS Nano* XXXX.
- 467 Reis PP, Tokar T, Goswami RS, Xuan Y, Sukhai M, Seneda AL, Moz LES, Perez-Ordonez B,
468 Simpson C, Goldstein D, Brown D, Gilbert R, Gullane P, Irish J, Jurisica I, and Kamel-Reid S.
469 2020. A 4-gene signature from histologically normal surgical margins predicts local recurrence in
470 patients with oral carcinoma: clinical validation. *Sci Rep* 10:1713. 10.1038/s41598-020-58688-y
- 471 Sarquis M, Marx SJ, Beckers A, Bradwell AR, Simonds WF, Bicalho MAC, Daly AF, Beta D,
472 Friedman E, and De Marco L. 2019. Long-term remission of disseminated parathyroid cancer
473 following immunotherapy. *Endocrine* 67:204-208. 10.1007/s12020-019-02136-z
- 474 Schafer ST, Paquola ACM, Stern S, Gosselin D, Ku M, Pena M, Kuret TJM, Liyanage M, Mansour
475 AA, Jaeger BN, Marchetto MC, Glass CK, Mertens J, and Gage FH. 2019. Pathological priming
476 causes developmental gene network heterochronicity in autistic subject-derived neurons. *Nature*
477 *Neuroscience* 22:243-255. 10.1038/s41593-018-0295-x
- 478 Shi S, Ye S, Mao J, Ru Y, Lu Y, Wu X, Xu M, Zhu T, Wang Y, Chen Y, Tang X, and Xi Y. 2020.
479 CMA1 is potent prognostic marker and associates with immune infiltration in gastric cancer.
480 *Autoimmunity*:1-8. 10.1080/08916934.2020.1735371
- 481 Sun W, Kuang XL, Liu YP, Tian LF, Yan XX, and Xu W. Crystal structure of the N-terminal
482 domain of human CDC73 and its implications for the hyperparathyroidism-jaw tumor (HPT-JT)
483 syndrome. *Scientific Reports*.
- 484 Szopa W, Burley TA, Kramer-Marek G, and Kaspera W. 2017. Diagnostic and Therapeutic
485 Biomarkers in Glioblastoma: Current Status and Future Perspectives. *Biomed Res Int*

- 486 2017:8013575. 10.1155/2017/8013575
- 487 Tan AC, Ashley DM, López G, Malinzak M, and Khasraw M. 2020. Management of glioblastoma:
488 State of the art and future directions. *CA A Cancer Journal for Clinicians* 70.
- 489 Tij A, Pr A, Acbc D, Is A, e FMMbcd, Rk F, Tka G, Dszbc H, Mkbc D, and Rm I. 2021. Frontiers
490 in the treatment of glioblastoma: Past, present and emerging - ScienceDirect. *Advanced Drug*
491 *Delivery Reviews*.
- 492 Tingting, Long, Zijng, Liu, Xing, Zhou, Shuang, Yu, Hui, and Tian. 2019. Identification of
493 differentially expressed genes and enriched pathways in lung cancer using bioinformatics analysis.
494 *Molecular Medicine Reports*.
- 495 Tonry C. 2020. Clinical proteomics for prostate cancer: understanding prostate cancer pathology
496 and protein biomarkers for improved disease management. *Clinical Proteomics* 17.
- 497 Tripathi S, Pohl Marie O, Zhou Y, Rodriguez-Frandsen A, Wang G, Stein David A, Moulton
498 Hong M, DeJesus P, Che J, Mulder Lubbertus CF, Yángüez E, Andenmatten D, Pache L,
499 Manicassamy B, Albrecht Randy A, Gonzalez Maria G, Nguyen Q, Brass A, Elledge S, White M,
500 Shapira S, Hacohen N, Karlas A, Meyer Thomas F, Shales M, Gatorano A, Johnson Jeffrey R,
501 Jang G, Johnson T, Verschuere E, Sanders D, Krogan N, Shaw M, König R, Stertz S, García-
502 Sastre A, and Chanda Sumit K. 2015. Meta- and Orthogonal Integration of Influenza “OMICs”
503 Data Defines a Role for UBR4 in Virus Budding. *Cell Host & Microbe* 18:723-735.
504 10.1016/j.chom.2015.11.002
- 505 Wang W, Xing H, Huang C, Pan H, and Li D. 2020. Identification of pancreatic cancer type related
506 factors by Weighted Gene Co-Expression Network Analysis. *Med Oncol* 37:33. 10.1007/s12032-
507 020-1339-0
- 508 Wu J, Su HK, Yu ZH, Xi SY, Guo CC, Hu ZY, Qu Y, Cai HP, Zhao YY, Zhao HF, Chen FR,
509 Huang YF, To ST, Feng BH, Sai K, Chen ZP, and Wang J. 2020. Skp2 modulates proliferation,
510 senescence and tumorigenesis of glioma. *Cancer Cell Int* 20:71. 10.1186/s12935-020-1144-z
- 511 Xing Z-y, Sun L-g, and Guo W-j. 2015. Elevated expression of Notch-1 and EGFR induced
512 apoptosis in glioblastoma multiforme patients. *Clinical Neurology and Neurosurgery* 131:54-58.
513 10.1016/j.clineuro.2015.01.018
- 514 Zhang B, and Horvath S. 2005. A general framework for weighted gene co-expression network
515 analysis. *Stat Appl Genet Mol Biol* 4:Article17. 10.2202/1544-6115.1128
- 516 Zhang L, Zhang Z, and Yu Z. 2019. Identification of a novel glycolysis-related gene signature for
517 predicting metastasis and survival in patients with lung adenocarcinoma. *J Transl Med* 17:423.
518 10.1186/s12967-019-02173-2
- 519 Zheng W, Zou Z, Lin S, Chen X, Wang F, Li X, and Dai J. 2018. Identification and functional
520 analysis of spermatogenesis-associated gene modules in azoospermia by weighted gene
521 coexpression network analysis. *Journal of Cellular Biochemistry* 120:3934-3944.
522 10.1002/jcb.27677
- 523 Zhou Z, Cheng Y, Jiang Y, Liu S, Zhang M, Liu J, and Zhao Q. 2018. Ten hub genes associated
524 with progression and prognosis of pancreatic carcinoma identified by co-expression analysis.

525 *International Journal of Biological Sciences* 14:124-136. 10.7150/ijbs.22619

526 Zucchini C, Strippoli P, Biolchi A, Solmi R, Lenzi L, D'Addabbo P, Carinci P, and Valvassori L.
527 2003. The human TruB family of pseudouridine synthase genes, including the Dyskeratosis
528 Congenita 1 gene and the novel member TRUB1. *Int J Mol Med* 11:697-704.

529 Zurlo G, and Zhang Q. 2020. Adenylosuccinate lyase hydroxylation contributes to triple negative
530 breast cancer via the activation of cMYC. *Mol Cell Oncol* 7:1707045.
531 10.1080/23723556.2019.1707045

532

533

534

Figure Caption

535 **Fig. 1. Identification of gene co-expression modules.** (A) cluster samples to detect outliers. All
536 samples are located in the cluster and pass the critical threshold at the same time. The green
537 highlighting means that the samples are in strong trait relationships established by correlation
538 analyses. (B) The scale-free fit index was analyzed under the background of different soft-
539 thresholding power (β). (C) Analyze average connectivity when using different soft-thresholding
540 powers. (D) Dendrogram clustering of all genomic genes in GBM samples. (E) Heatmap of co-
541 expressed genes. Different modules on the X and Y axis have different colors. The connection
542 degree of different modules is indicated by the yellow intensity.

543 **Fig. 2. Correlation of modules and clinical traits.** (A) Module intrinsic genes and relapse
544 Heatmap of the correlation between. (B) Scatter plot of the correlation between the darkturquoise
545 module and relapse. All modules can be correlated with genes, and all continuous traits can be
546 correlated with gene expression values. The two correlation matrices are combined and the vertical
547 coordinate is the Gene significance for luminal when the module of interest is specified for
548 analysis. (C) Enrichment analysis of the function and pathway of the darkturquoise module. The
549 rich biological process terms in the selected modules are described as interactive networks and
550 listed according to their P-value. The size of the dots represents the number of genes that are co-
551 expressed, the larger the dot, the more genes are co-expressed, presumably the more important
552 they are and the more important they are as core genes in the network graph. Each node is a gene.
553 The size of the node means degree of gene enrichment. Set $P < 0.01$ as the cutoff criterion. Enrich
554 the term network, colored with cluster-ID, where nodes sharing the same cluster ID are usually
555 close to each other.

556 **Fig. 3. The Kaplan-Meier survival curve can evaluate the prognostic performance of core**
557 **genes based on the expression status of selected biomarkers in the database.** (A) DARS. (B)
558 GDI2. (C) P4HA2. (D) TRUB1. All patients in each group were divided into high expression group
559 and low expression group by gene expression. The cutoff for low versus high expression is 3-fold
560 expression of controls.

561 **Fig. 4. Gene co-expression.** (A-H) In the TCGA dataset, selected the mRNA expression levels of
562 DARS / GDI2 / P4HA2 / TRUB1 related genes, analyzed the correlation of these genes through
563 R, and visualize them with the circus and heatmap graph. (I-L) The four genes with the highest
564 correlation with DARS / GDI2 / P4HA2 / TRUB1, drew scatter plots.

565 **Fig. 5. Drug sensitivity analysis.** (A) The role of DARS/GDI2/P4HA2/TRUB1 in the famous
566 cancer related pathways (GSCALite). The size of an area in the pie chart represents the extent of
567 the role of DARS/GDI2/P4HA2/TRUB1 in the well-known cancer-related pathway (GSCALite).
568 (B) In the GDSC training set, high expression of DARS/GDI2/P4HA2/TRUB1 was inferred to be
569 less sensitive to commonly used chemotherapy drugs. The test for association between paired
570 samples used Pearson's correlation coefficient. Two-tailed statistical P values were calculated by
571 a two-sample Mann-Whitney test or Student's t test when appropriate.

572 **Fig. 6. Genetic and transcriptional changes and connections with immune cell populations.**
573 (A) Correlation of DARS/GDI2/P4HA2/TRUB1 expression with immune infiltration level in
574 GBM. (B) DARS/GDI2/P4HA2/TRUB1 copy number alterations (CNV) affects the level of

575 infiltration of B cells, CD8+ T cells, CD4+T celles, Macrophages, Neutrophils, and Dendritic cells
576 in GBM.

577 **Fig. 7. Genomic alterations of DARS/GDI2/P4HA2/TRUB1 in GBM.** OncoPrint of
578 DARS/GDI2/P4HA2/TRUB1 alterations in GBM cohort. The different types of genetic alterations
579 are highlighted in different colors. Expression profiles of mRNAs showing different expression
580 (≥ 3 -fold) compared to control were considered to be mRNA high, and vice versa for low.

581 **Fig. 8. GSVA analysis. GSVA of DARS/GDI2/P4HA2/TRUB1 gene sets in GBM.** (A) DARS.
582 (B) GDI2. (C) P4HA2. (D) TRUB1. A t value > 1 or < -1 represents statistically significant
583 changes.

584

Figure 1

Identification of gene co-expression modules.

(A) cluster samples to detect outliers. All samples are located in the cluster and pass the critical threshold at the same time. The green highlighting means that the samples are in strong trait relationships established by correlation analyses. (B) The scale-free fit index was analyzed under the background of different soft-thresholding power (β). (C) Analyze average connectivity when using different soft-thresholding powers. (D) Dendrogram clustering of all genomic genes in GBM samples. (E) Heatmap of co-expressed genes. Different modules on the X and Y axis have different colors. The connection degree of different modules is indicated by the yellow intensity.

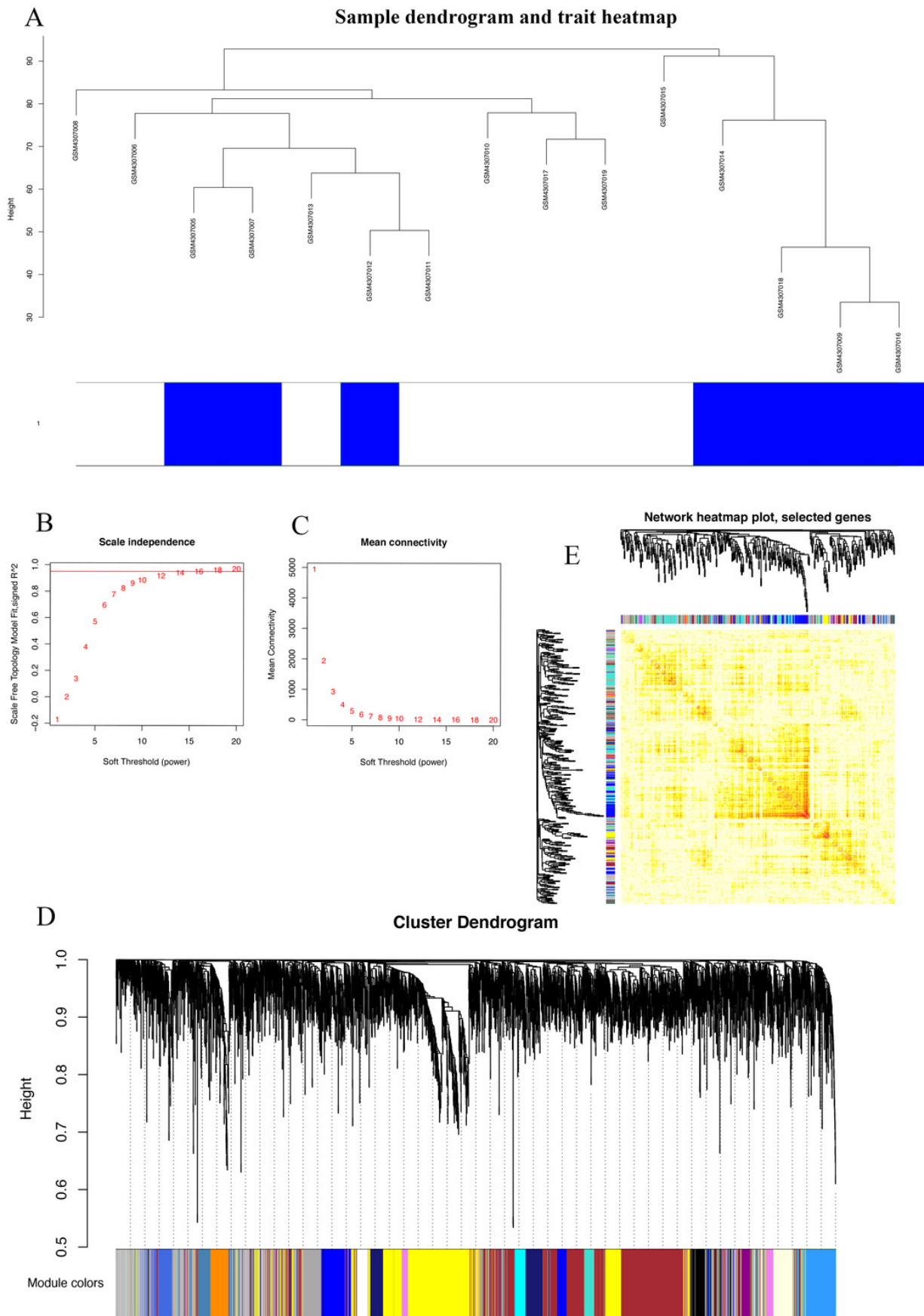


Figure 2

Correlation of modules and clinical traits.

(A) Module intrinsic genes and relapse Heatmap of the correlation between. (B) Scatter plot of the correlation between the darkturquoise module and relapse. All modules can be correlated with genes, and all continuous traits can be correlated with gene expression values. The two correlation matrices are combined and the vertical coordinate is the Gene significance for luminal when the module of interest is specified for analysis. (C) Enrichment analysis of the function and pathway of the darkturquoise module. The rich biological process terms in the selected modules are described as interactive networks and listed according to their P-value. The size of the dots represents the number of genes that are co-expressed, the larger the dot, the more genes are co-expressed, presumably the more important they are and the more important they are as core genes in the network graph. Each node is a gene. The size of the node means degree of gene enrichment. Set $P < 0.01$ as the cutoff criterion. Enrich the term network, colored with cluster-ID, where nodes sharing the same cluster ID are usually close to each other.

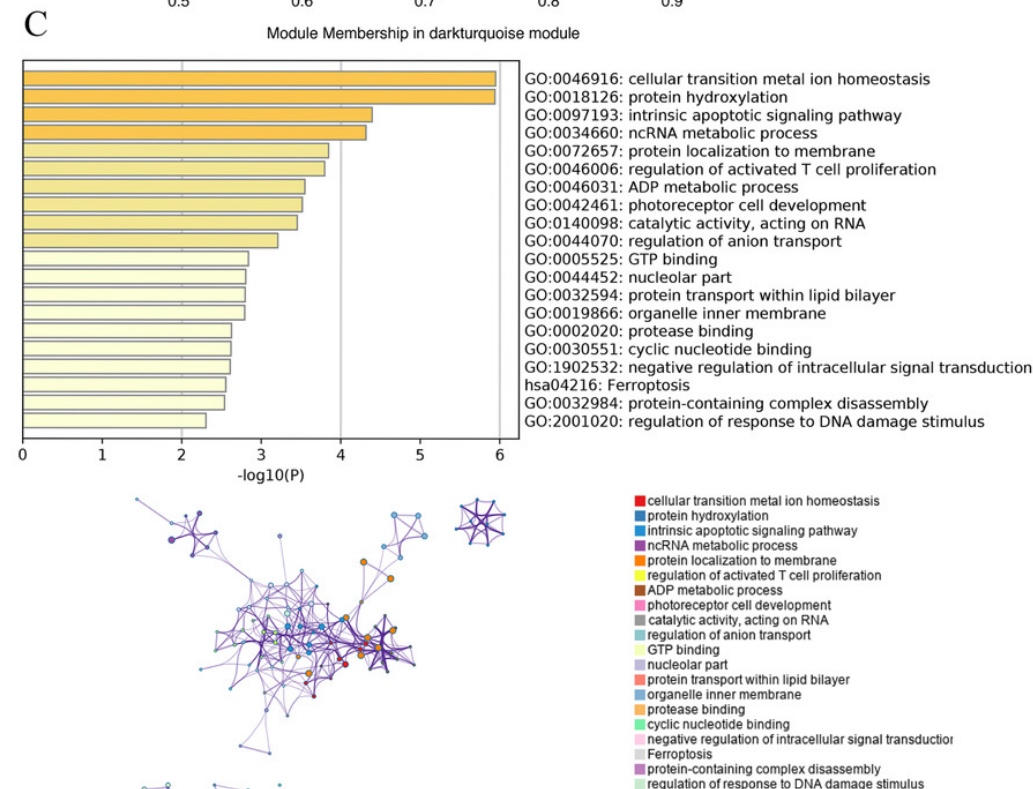
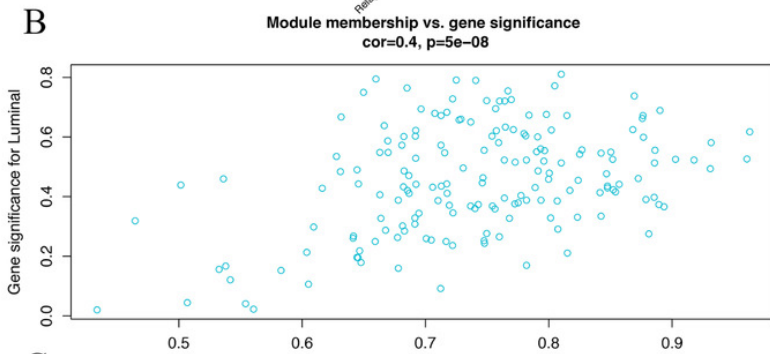
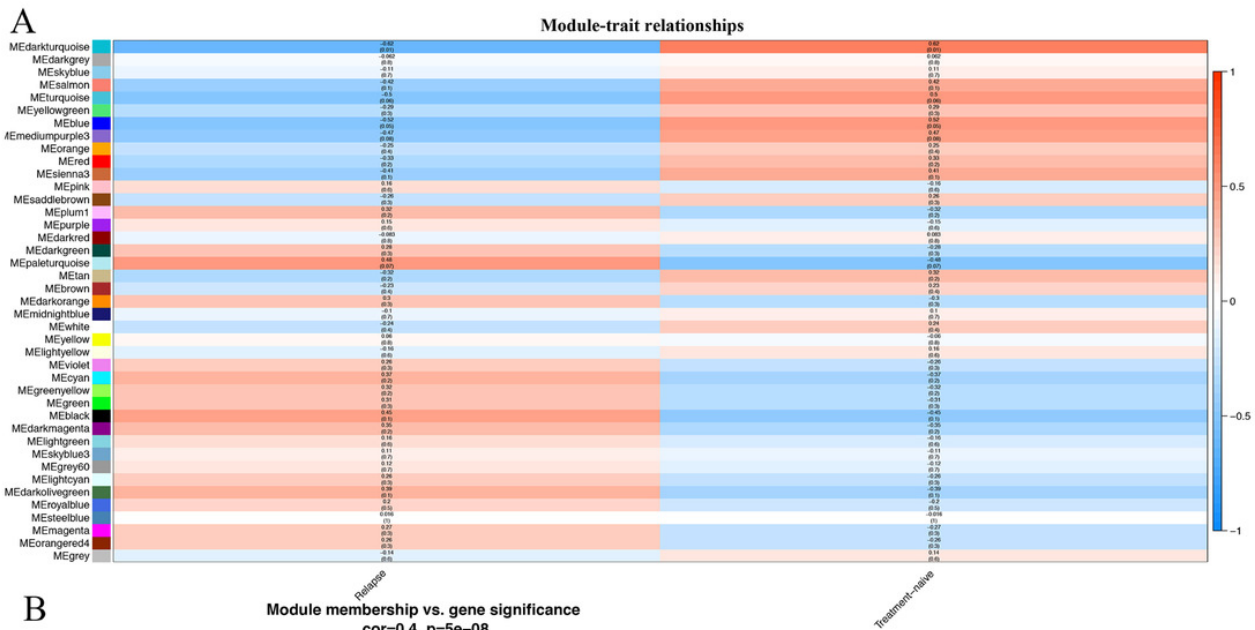


Figure 3

The Kaplan-Meier survival curve can evaluate the prognostic performance of core genes based on the expression status of selected biomarkers in the database.

(A) DARS. (B) GDI2. (C) P4HA2. (D)TRUB1. All patients in each group were divided into high expression group and low expression group by gene expression. The cutoff for low versus high expression is 3-fold expression of controls.

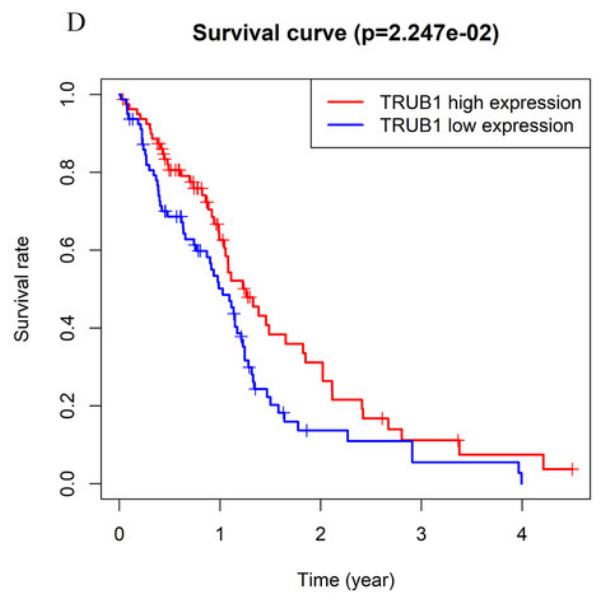
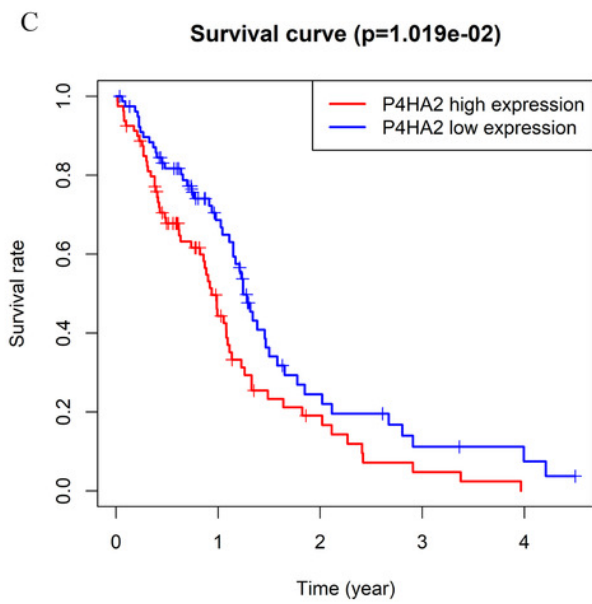
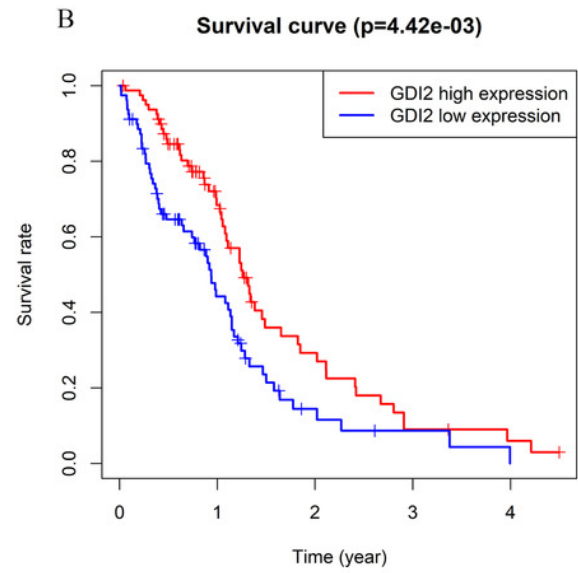
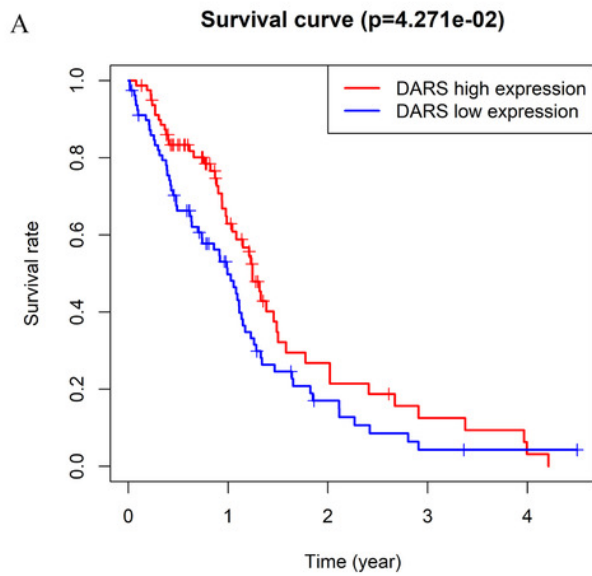


Figure 4

Gene co-expression.

(A-H) In the TCGA dataset, selected the mRNA expression levels of DARS / GDI2 / P4HA2 / TRUB1 related genes, analyzed the correlation of these genes through R, and visualize them with the circus and heatmap graph. (I-L) The four genes with the highest correlation with DARS / GDI2 / P4HA2 / TRUB1, drew scatter plots.

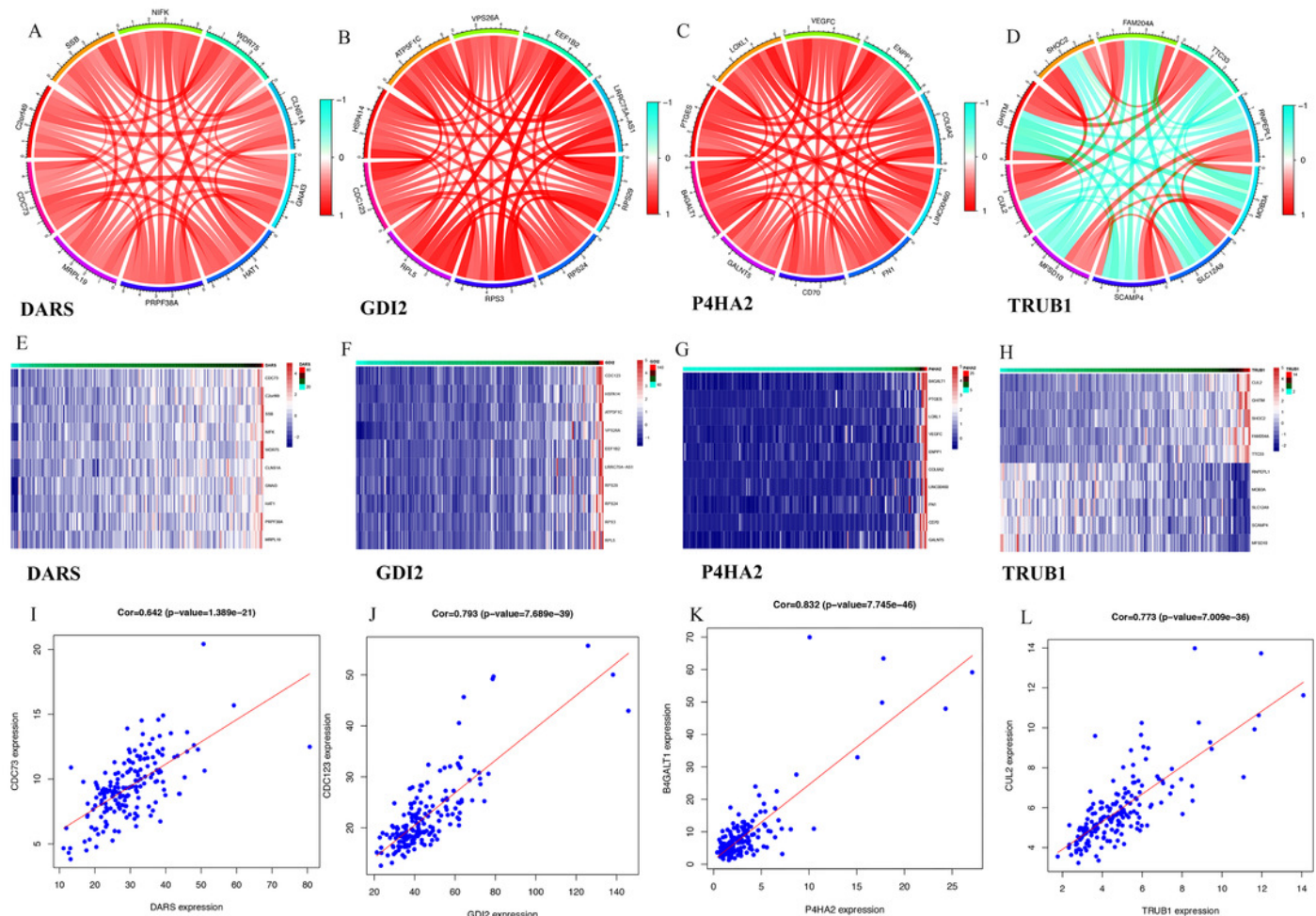


Figure 5

Drug sensitivity analysis.

(A) The role of DARS/GDI2/P4HA2/TRUB1 in the famous cancer related pathways (GSCALite). The size of an area in the pie chart represents the extent of the role of DARS/GDI2/P4HA2/TRUB1 in the well-known cancer-related pathway (GSCALite). (B) In the GDSC training set, high expression of DARS/GDI2/P4HA2/TRUB1 was inferred to be less sensitive to commonly used chemotherapy drugs. The test for association between paired samples used Pearson's correlation coefficient. Two-tailed statistical P values were calculated by a two-sample Mann-Whitney test or Student's t test when appropriate.

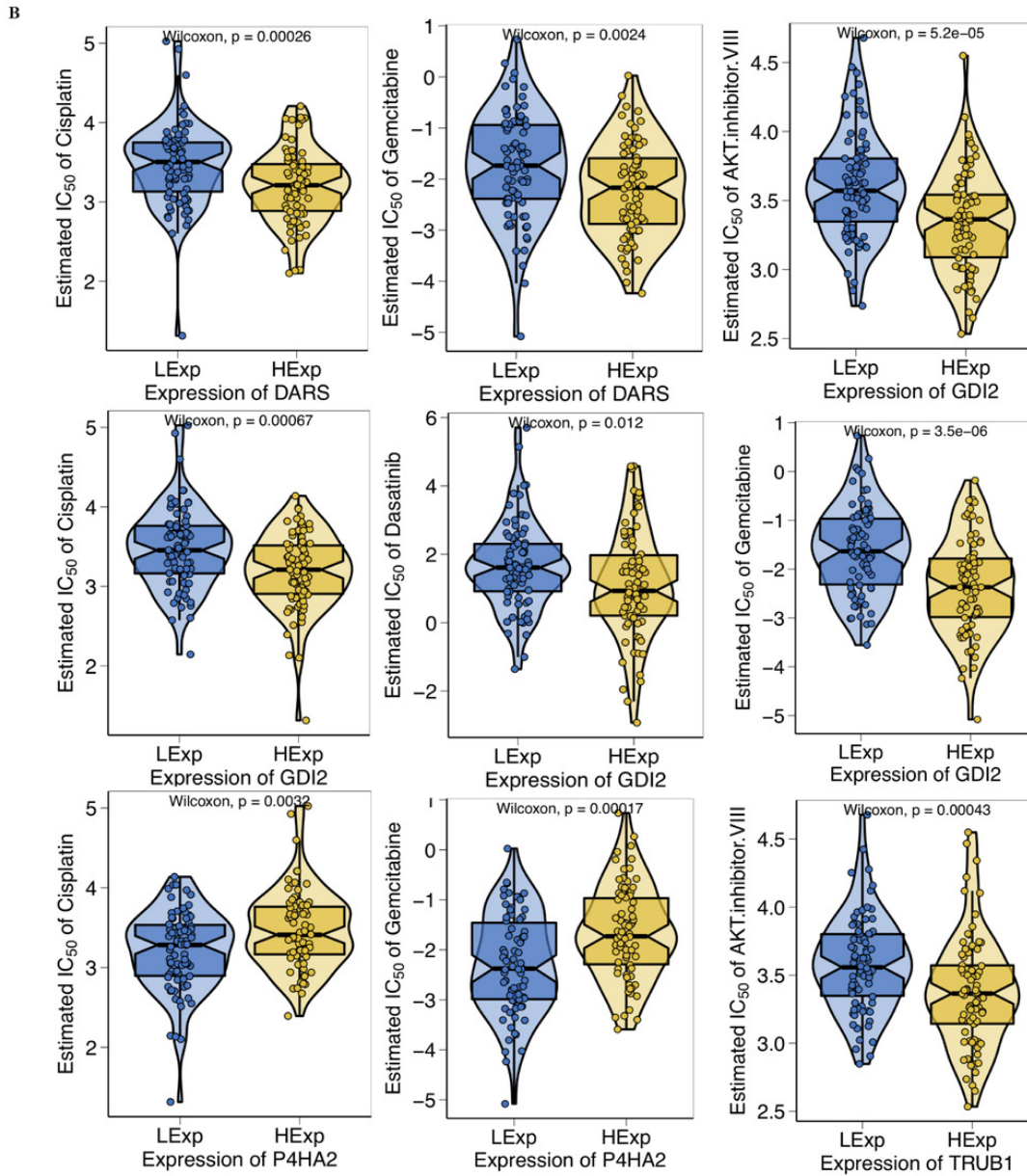
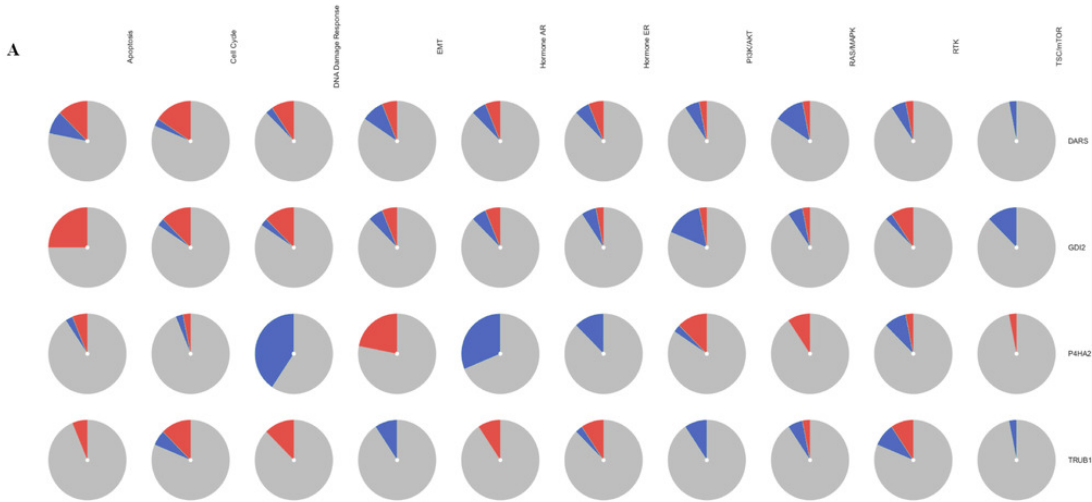


Figure 6

Genetic and transcriptional changes and connections with immune cell populations.

(A) Correlation of DARS/GDI2/P4HA2/TRUB1 expression with immune infiltration level in GBM.

(B) DARS/GDI2/P4HA2/TRUB1 copy number alterations (CNV) affects the level of infiltration of B cells, CD8+ T cells, CD4+T cells, Macrophages, Neutrophils, and Dendritic cells in GBM.

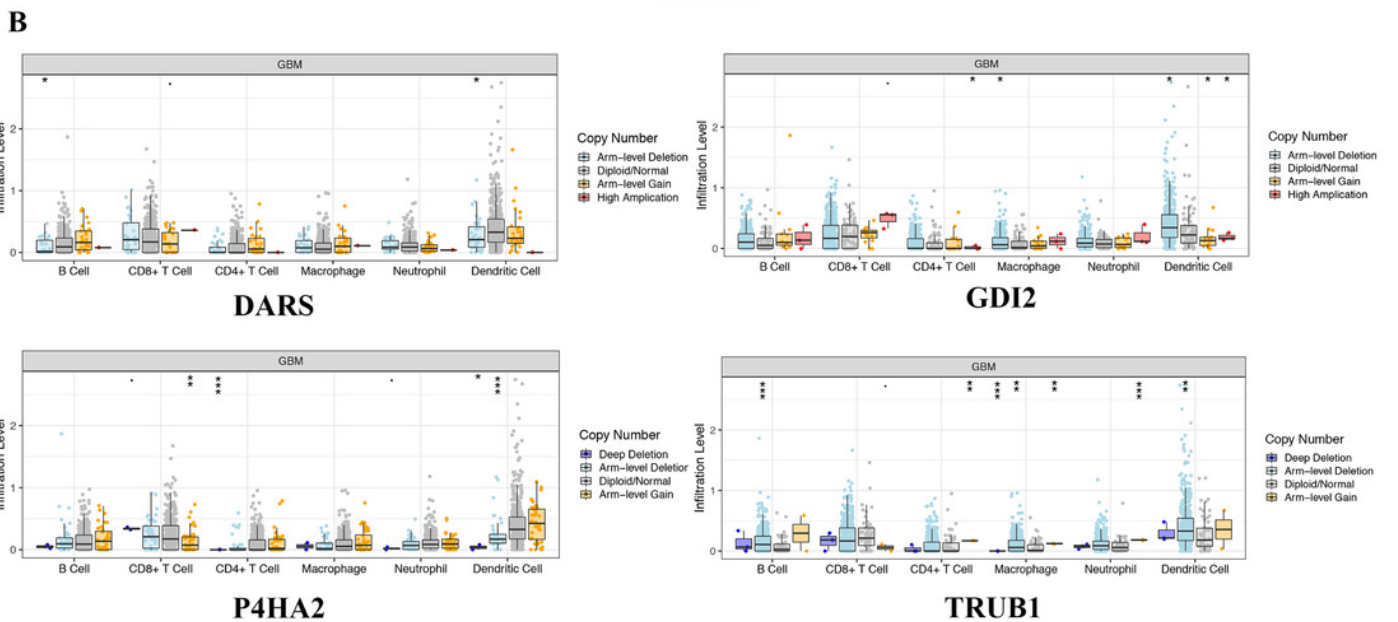
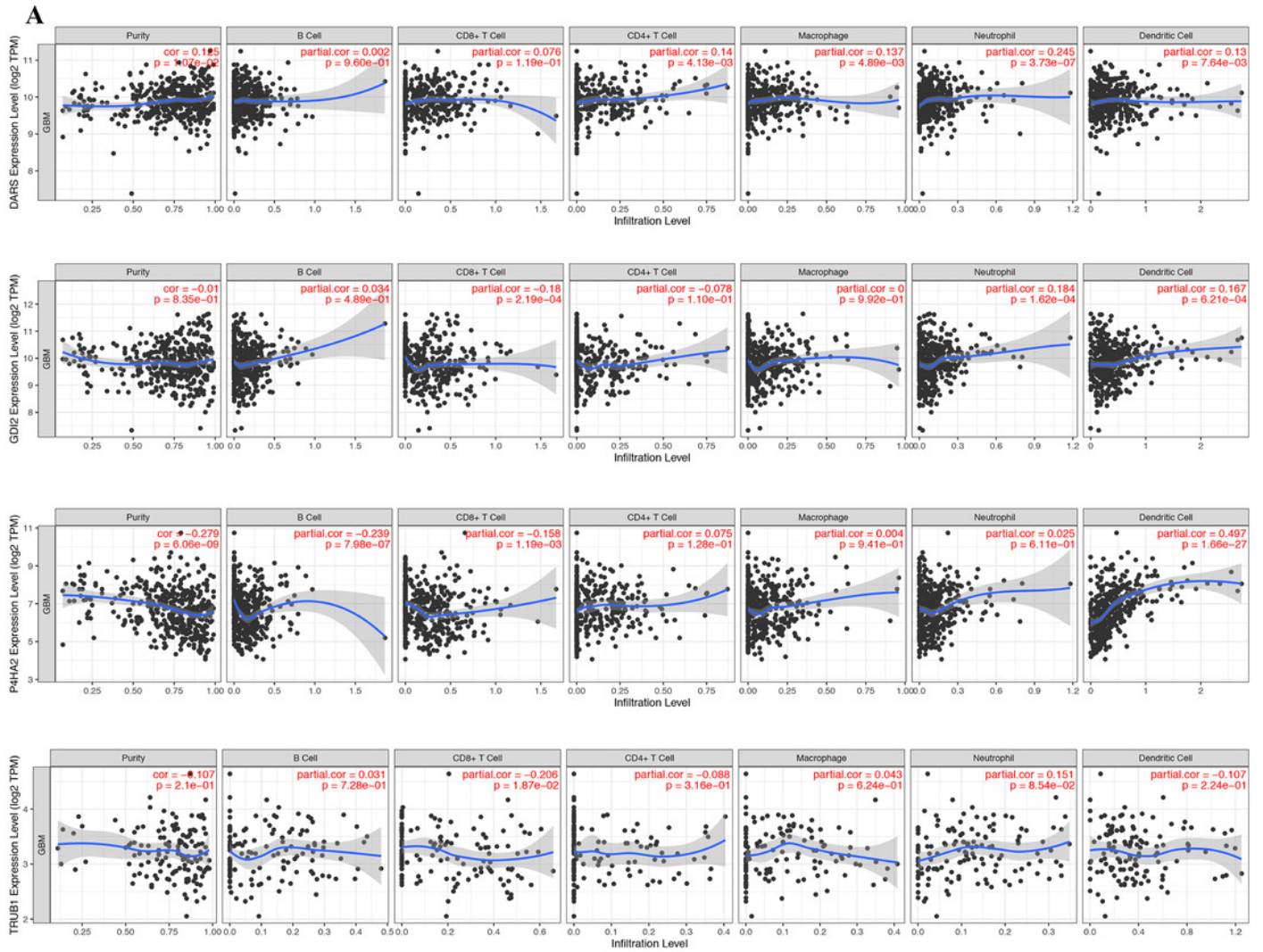


Figure 7

Genomic alterations of DARS/GDI2/P4HA2/TRUB1 in GBM.

OncoPrint of DARS/GDI2/P4HA2/TRUB1 alterations in GBM cohort. The different types of genetic alterations are highlighted in different colors. Expression profiles of mRNAs showing different expression (≥ 3 -fold) compared to control were considered to be mRNA high, and vice versa for low.

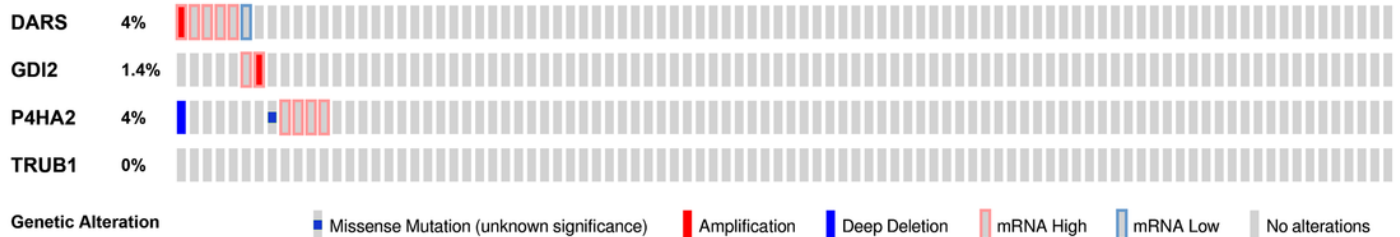
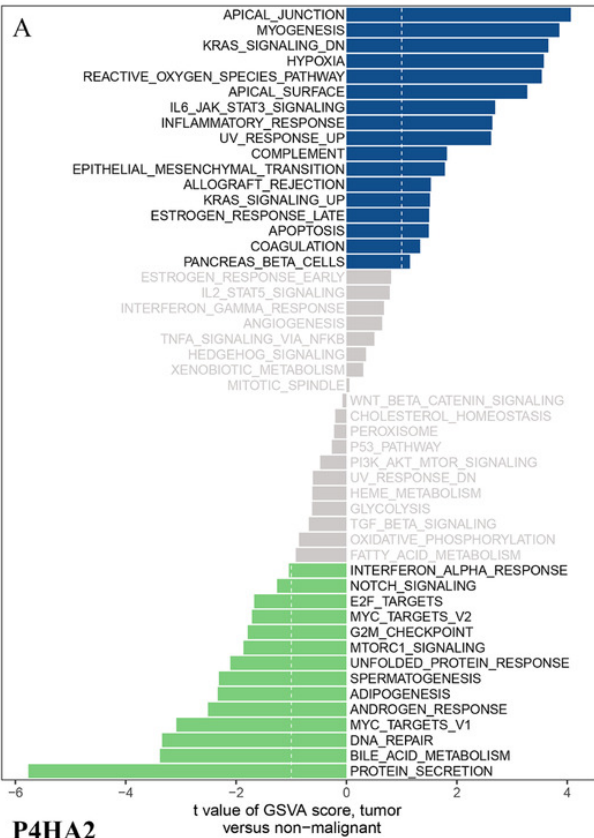


Figure 8

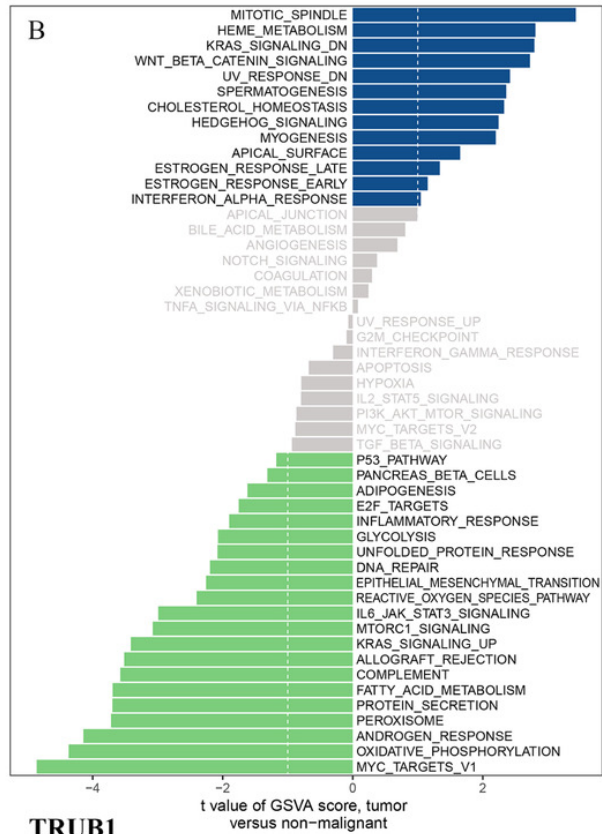
Fig. 8. GSVA analysis. GSVA of DARS/GDI2/P4HA2/TRUB1 gene sets in GBM.

(A) DARS. (B) GDI2. (C) P4HA2. (D) TRUB1. A t value > 1 or < -1 represents statistically significant changes.

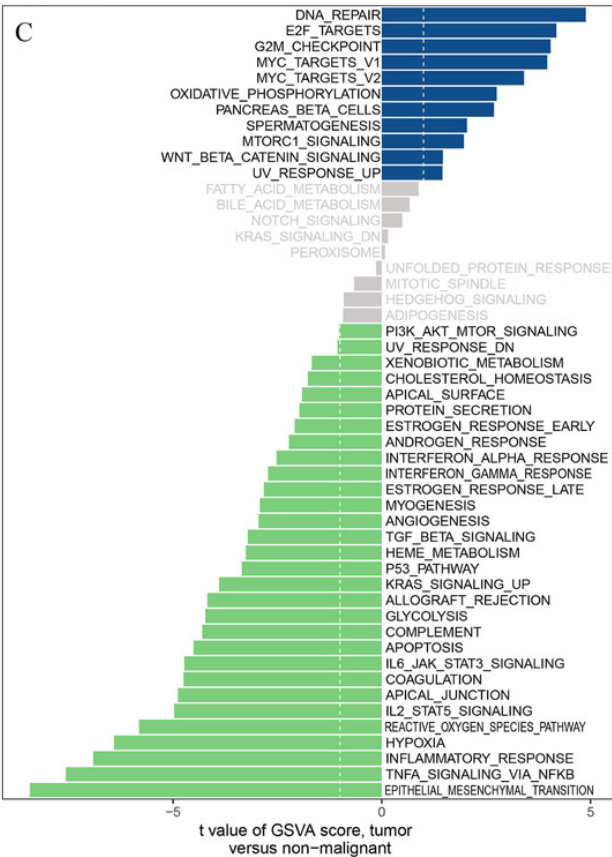
DARS



GDI2



P4HA2



TRUB1

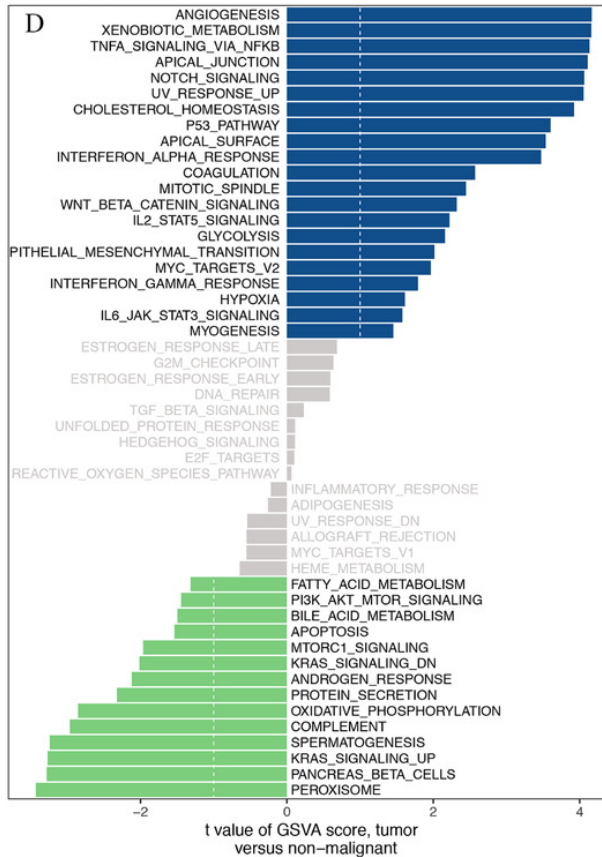


Table 1 (on next page)

Table1: Statistics of genes in darkturquoise modules.

Table1 Statistics of genes in darkturquoise modules.

1 Table1 Statistics of genes in darkturquoise modules.

2

Gene	P value
TRUB1	2.25E-02
P4HA2	1.02E-02
DARS	4.27E-02
FKBP1B	6.13E-03
NRL	2.20E-02
CORO6	1.83E-02
LRRC43	4.65E-02
GAS6	3.63E-02
SPAG4	2.07E-03
PRKAR2B	1.48E-02
CAMSAP2	1.31E-02
CD24	2.52E-02
GDI2	4.42E-03
DLEU1	1.45E-02

3